# Large-Eddy Simulation of Stratification Effects on Dispersion in Urban Environments

Zheng-Tong Xie[*]

*Aeronautics and Astronautics, Faculty of Engineering and the Environment*
*University of Southampton, Southampton, SO17 1BJ, UK*

Paul Hayden

*Environmental Flow Research Laboratory, Faculty of Engineering and Physical Sciences,*
*University of Surrey, Guildford, GU2 7XH, UK*

Curtis R. Wood[1]

*Finnish Meteorological Institute, Erik Palmnin aukio 1, 00101 Helsinki, Finland.*

## Abstract

This paper investigates thermal stratification effects on dispersion of approach flows in urban environments. A generic urban-type geometry, i.e. a group of staggered cubes, was taken as the first test case. The DAPPLE site, which was about a one-km$^2$ region near the intersection of Marylebone Road and Gloucester Place in central London, was taken as the second test case. Only weakly unstable conditions (i.e. bulk Richardson number $R_b \geq$ -0.2) of approach flows were considered, with adiabatic boundary conditions at the ground and building surfaces. A number of numerical experiments including with various Richardson numbers were performed. It was found that the modelled mean concentration for $R_b = -0.1$ gave the best agreement with the field data at all DAPPLE stations. This suggests that stratification effects on dispersion in weakly unstable conditions (e.g. in London) are not negligible.

*Keywords:* stability, scalar, building, CFD, weather-scale

[*]Email: z.xie@soton.ac.uk
[1]Former institute:Department of Meteorology, University of Reading, Reading, RG6 6BB, UK

## 1. INTRODUCTION

It is of great interest to accurately model scalar dispersion over short ranges (<1 km) in full-scale urban environments. Large-eddy simulation (LES) is a promising tool for this purpose and is particularly useful for modelling the genuine unsteadiness of plume dispersion (Niceno and Hanjalić, 2002; Tseng et al., 2006; Xie et al., 2004), e.g. the meandering of the plume. However, a few issues need to be solved.

For example, it is known that the mean concentration obtained from small scale physical or numerical models can be about one order greater than that obtained in field experiments (Cheng and Robins, 2004; Xie and Castro, 2009). The discrepancy might be attributed to: (I) the variation of wind direction and magnitude because of the weather conditions; (II) thermal buoyancy effects of approach flows and local heat transfer from/to buildings; (III) small roughness elements and (IV) Reynolds number effects.

In Xie (2011) it is reported that the dispersion in an urban region was found sensitive to the variation of wind direction. Study on (I) was reported in Xie (2011), in which DAPPLE wind data (Wood et al., 2009, 2010) measured on BT Tower at 190 m above street level were processed - turbulent eddies with scales below one minute were re-generated using the recently developed approach (Xie and Castro, 2008) - and were used to drive the LES. The DAPPLE site (Arnold et al., 2004) is approximately 1 km region near the intersection of Marylebone Road and Gloucester Place in central London. When using the BT Tower data to generate inlet boundary conditions to drive the LES, the predicted dispersion in the near field (i.e. less than 400 m) was in better agreement with the field measurements than in steady inlet conditions. Using realistic wind conditions improves the LES prediction significantly. However, in the far field (i.e. greater than 400 m) the improvement of the LES prediction was marginal. The discrepancy between LES and field data remains significant in the far field.

Other factors, which were not considered in the previous paper (Xie, 2011), are likely to blame. It is known that the thermal stability of urban environments is generally weaker than that of rural environments because of the greater friction velocity $u_*$ over urban regions (Britter and Hanna, 2003). This might be one reason that there are so far not many publications of modelling of urban-stability effect on dispersion. However this has recently attracted more attention. Many of these research investigated thermal stratification and its effects on flows in two-dimensional street canyons (Uehara et al., 2000; Liu et al., 2003; Louka et al., 2002). Richards et al. (2006) and Boppana et al. (2012) investigated the thermal

effects within the vicinity of a heated cube in a deep surface layer over a rough wall. Kanda and Moriizumi (2009) studied momentum and heat transfer over a group of large blocks in the COSMO experiments. It is to be noted that most of these works are wind tunnel or field experiments. Niceno and Hanjalić (2002) used large-eddy simulation (LES) to study heat transfer from a group of cubes with only one cube heated at a very low Richardson number with negligible buoyancy effect. They demonstrated that LES is potentially a promising tool for heat transfer applications but at a cost of a very fine near-wall resolution.

It is still a big challenge to use LES for flows and heat transfer at high Reynolds number and Richardson number. One issue is that an accurate calculation for the thin thermal layers on the solid walls is required (Boppana et al., 2010). Any attempt to resolve such layers for a realistic Reynolds number is too expensive, while an appropriate thermal wall model is not available yet. Therefore, as an initial work stratification effects on turbulent flows and dispersion of approach flows was investigated, while the building surfaces and ground were considered as adiabatic walls.

In the following, Section 2 briefly presents the governing equations of the LES and numerical details, including geometry, mesh and boundary conditions. Section 3 presents LES results of flows under weakly unstable or stable conditions over a group of staggered cubes. Section 4 presents a comparison of LES data over DAPPLE site between neutral condition and weakly unstable condition, and a validation using wind tunnel and field data. Conclusions and final remarks are presented in Section 5.

## 2. Governing Equations of flows and scalar dispersion

Large-eddy simulation (LES) resolves only the large-scale fluid motions and models the subgrid-scale (SGS) motions through filtering the Navier-Stokes equations. The SGS eddies provide the high frequency content at the upper end of the spectrum and thus, provided the grid is fine enough, contribute little to the total turbulent kinetic energy. To ensure a largely self-contained paper, a brief description of the governing equations is given here. More details for the flow and scalar can be found in Xie and Castro (2006), hereafter denoted by XC.

The filtered continuity and Navier-Stokes equations are written as follows,

$$\frac{\partial \bar{u}_i}{\partial x_i} = 0$$
$$\frac{\partial \bar{u}_i}{\partial t} + \frac{\partial \bar{u}_i \bar{u}_j}{\partial x_j} = -\frac{1}{\rho}\left(\frac{\partial \bar{p}}{\partial x_i}\right) + \frac{\partial}{\partial x_j}\left(\frac{\tau_{ij}}{\rho} + \nu\frac{\partial \bar{u}_i}{\partial x_j}\right). \tag{1}$$

The dynamical quantities, $\bar{u}_i, \bar{p}$ are resolved-scale (filtered) velocity and pressure respectively. $\rho$ and $\nu$ are respectively density and kinematic molecular viscosity. $\tau_{ij}$ is the subgrid-scale (SGS) Reynolds stress. The Smagorinsky SGS model was used with the constant $C_s = 0.1$,

$$\tau_{ij} - \delta_{ij}\tau_{kk}/3 = 2\rho(C_s\Delta)^2(2\bar{s}_{mn}\,\bar{s}_{mn})^{1/2}\bar{s}_{ij}, \tag{2}$$

where $\bar{s}_{ij} = \frac{1}{2}(\frac{\partial \bar{u}_i}{\partial x_j} + \frac{\partial \bar{u}_j}{\partial x_i})$; $\Delta$ is taken as the cubic root of the cell volume; $\tau_{kk}$ is modelled according to a closure similar to the one devised by Yoshizawa (1986). $\delta_{ij}$ is the Kronecker-delta. In the near-wall region, the Lilly damping function was also applied.

The filtered scalar transport equation is written as follows,

$$\frac{\partial \bar{c}}{\partial t} + \frac{\partial \bar{u}_j \bar{c}}{\partial x_j} = \frac{\partial}{\partial x_j}\left(q_j + K_m\frac{\partial \bar{c}}{\partial x_j}\right) + S, \tag{3}$$

where $\bar{c}$ is resolved-scale (filtered) scalar. $K_m$ is the molecular diffusivity. $q_j = K_s\frac{\partial \bar{c}}{\partial x_j}$ is the subgrid-scale (SGS) scalar flux, where $K_s$ is the subgrid turbulent diffusivity. $S$ is the source term - a function of space and time. Up to now most studies for concentration dispersion problems have applied a subgrid eddy viscosity combined with a subgrid scale Schmidt number, which are set as constant or calculated dynamically. In the present study, we adopt this approach using a constant subgrid scale Schmidt number of unity.

$$K_s = \nu_s/Sc_s,$$

where $\nu_s$ is the subgrid viscosity calculated in Eq. 2, and $Sc_s$ is the subgrid Schmidt number.

The filtered temperature transport equation is written as follows,

$$\frac{\partial \bar{\theta}}{\partial t} + \frac{\partial \bar{u}_j \bar{\theta}}{\partial x_j} = \frac{\partial}{\partial x_j}\left((d_s + d_m)\frac{\partial \bar{\theta}}{\partial x_j}\right), \tag{4}$$

where $\bar{\theta}$ is resolved-scale (filtered) absolute temperature. $d_s$, $d_m$ are subgrid and molecular eddy diffusivity respectively. The former is modelled using a subgrid eddy viscosity combined with a constant subgrid scale Prandtl number of 0.9 as usual.

The entire LES model was implemented in the code described in Xie and Castro (2009). The discretisation for all terms in Eqs. 1-4 was second-order accurate in both space and time. A second order monotone advection and reconstruction scheme (MARS) for the convective terms in space were applied to solve Eqs. 3 and 4. The MARS is used to capture the sharp gradients at the edge of the scalar plume and to avoid generating spurious negative concentrations.

### 2.1. Inlet boundary conditions

Appropriate settings of inlet boundary conditions are crucial for LES. However, the available field and wind tunnel data are extremely sparse. Numerical experiments of LES were inevitably necessary to test the sensitivity of the results to the critical parameters. Since only weakly unstable or stable conditions were considered in the present paper, turbulence statistics data used in Xie and Castro (2008) and Xie and Castro (2009) for inflow conditions, which were fitted from wind tunnel measurements obtained in neutral conditions, were used to generate inflow conditions for Case A in §3 - and Case B in §4.

Temperature data of DAPPLE field experiments (Martin et al., 2010a) on 15/05/2003 were not available. The temperature profiles specified at inlet boundaries B1, B2 and B4 were approximately estimated by using Businger-Dyer relation for unstable conditions from BT Tower data obtained on 03/06/2004 (Martin et al., 2010b; Wood et al., 2009). We focus on numerical experiments investigating the effects of thermal stability of the approach flows by varying the bulk Richardson number $R_b$ number, rather than attempting to estimate an 'accurate' one. The $R_b$ is calculated as,

$$R_b = g\Delta\theta h/(\theta_a U_{ref}^2), \tag{5}$$

where $\Delta\theta$ is the difference between ground temperature $\theta_f$ and freestream temperature $\theta_a$; $g$ is acceleration due to gravity; $h$ is the average building height; $U_{ref}$ is the freestream velocity.

For Case A, the settings for the flows are the same as those in Xie and Castro (2008) with a Reynolds number approximately 3,000 based on the freestream velocity and the cube height. $R_b$ numbers -0.2, -0.1, 0, 0.1 and 0.2 of the approach flows were investigated. For Case B, a Reynolds number based on the

5
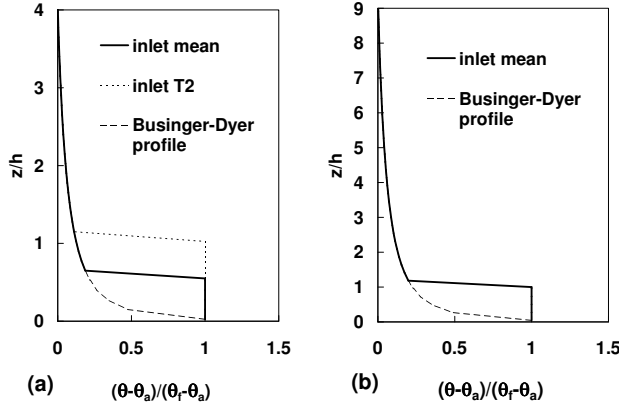
Figure 1: Dimensionless mean temperature profiles at inlet. (a) for case A; (b) for case B. $\theta_a$, freestream temperature; $\theta_f$, ground floor temperature; h cube height or mean building height.

freestream velocity and the mean building height of the wind tunnel model was about 18,000. The bulk Richardson number $R_b$ of the DAPPLE field experiments varied from -0.07 to -0.1 during 16:00-17:00 on 03/06/2004 , whilst it varied from -0.05 to -0.17 during 12:00 - 20:00 (Wood et al., 2009). The $R_b$ was estimated based on the wind speeds and temperatures measured at the BT Tower top and the roof of the 16-meter height Westminster Council House by the Marylebone Road and Gloucester Place intersection. A few numerical experiments (i.e. $R_b =$ -0.01, -0.03, -0.1, without local heating) were performed. For using the BT Tower data, the LES was initialised at 16:00 on 03/06/2004. The non-reactive tracer was released at 16:30 when the sampling was started and turned off at 16:45, but the sampling continued until 17:00, when at all sites the instantaneous concentration was zero (Martin et al., 2010b).

Fig. 1 shows dimensionless mean temperature $(\theta - \theta_a)/(\theta_f - \theta_a)$ at the inlet. The Businger-Dyer profiles are derived from Businger-Dyer relations (Stull, 1988, pp360-361). We noticed that the sharp peak in the near wall region of the original Businger-Dyer profile decayed rapidly when it was converted from the inlet into the domain without wall heating. It was assumed that for in the near wall region (i.e. $z/h \leq 0.55$) the temperature was well mixed and was approximated as a constant as shown in Fig. 1 (a) for case A. In addition, in Fig. 1 (a) it was assumed that within the canopy (i.e. $z/h \leq 1.0$) the temperature was approximated as a constant as a numerical experiment. In Fig. 1 (b) for case B the temperature was assumed constant within the canopy (i.e. $z/h \leq 1.0$).

6

Variances and integral length scales of temperature fluctuations are required for the generation of instantaneous temperature at the inlet. This procedure is similar to the turbulence generation in Xie and Castro (2008, 2009). Because measurements of temperature fluctuations are not always available, numerical experiments using various variances and integral length scales of the temperature fluctuations were conducted, which are detailed in §3 and §4.

## 3. Flow over a group of staggered cubes - Case A

Flows and heat transfer over a group of cubes mounted on a wall provides a good test case for validation of large-eddy simulation (LES) of urban flows (Pascheke et al., 2008; Boppana et al., 2010). The details of the parameters used for these calculations can be found in Xie and Castro (2008), in which LES with efficient inflow conditions was applied to calculate turbulent flows over a group of staggered wall-mounted cubes in neutral conditions. Here only a brief description of the computational domain and the boundary conditions is given. Figure 2 is a schematic view of the computational domain used for the Case A. It consists of eight rows of staggered cubes (four of the repeated units stacked in the stream-wise direction). It was found that converged turbulence statistics were produced in such a domain (Xie and Castro, 2008). The four vertical lines indicate data sampling locations and are subsequently denoted (from left to right) by 'behind row 1', 'behind row 3', 'behind row 5' and 'behind row 7'. These 4 stations all correspond to the P1 station in Figure 2b. Figure 2b shows a plan view of one repeated unit of the staggered wall-mounted cube array. The domain height was $4h$, where $h$ was defined as the cube height. The plan area density of the cubic array was 0.25. P0, P1, P2 and P3 denote the four typical data sampling locations. The synthetic inflow data was imposed at the inlet and zero-gradient outflow conditions at the outlet. At the top of the domain, stress free conditions were applied. Periodic boundary conditions were used in the lateral direction. Solid wall boundary conditions with a wall model were applied for all other boundaries (see details in XC). A uniform mesh of more than one million cells with $16 \times 16 \times 16$ grid points per cube was used, which was suggested by XC for sufficient accuracy in these kinds of flows.

Since only weakly thermal stratification were considered, the turbulence statistics and the integral length scales which were applied for the generation of the inflow data were the same as those in a neutral condition in Xie and Castro (2008). This helps to isolate the problem whether the thermal stratification (or temperature gradient) has an impact on turbulence and dispersion. Also note that the $U_m(z)$,

7
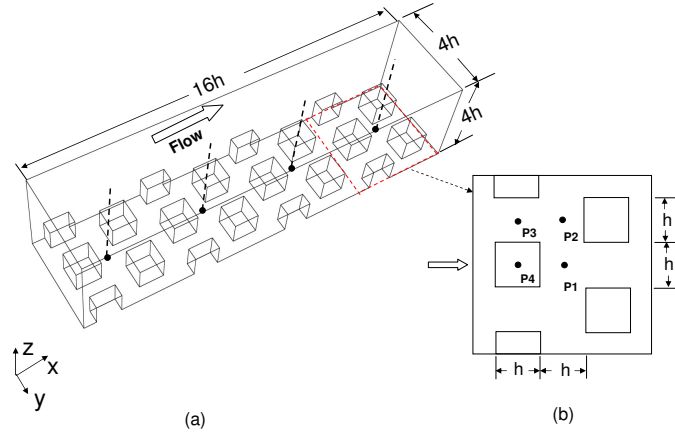
Figure 2: (a) Schematic view of the domain of a group of staggered cubes. (b) Plan view of one repeated unit. P1, P2, P3 and P4, four typical sampling stations.
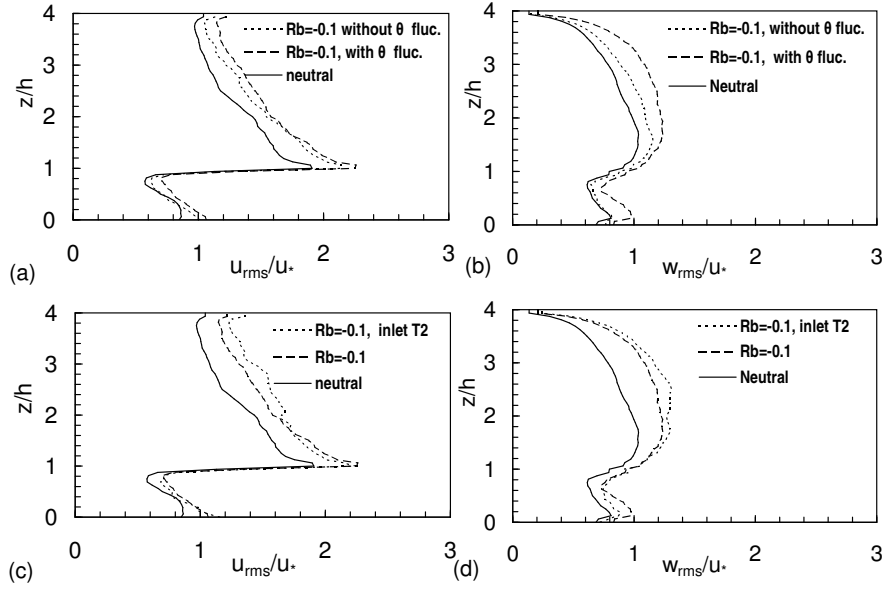


Figure 3: Sensitivity to inlet conditions. Effects of inlet temperature fluctuations (a, b) and shape of mean temperature profiles (c, d) on velocity fluctuation *rms* at station *P*1 behind row 7 (see Fig. 2). $u_*$, mean friction velocity.

8

$\overline{u'w'}$(z), $u_{rms}(z)$, $v_{rms}(z)$, $w_{rms}(z)$ profiles were not functions of $y$ for simplicity. This could easily be done but in practical cases it is unlikely that sufficient knowledge of such spanwise variations would be available to make it either sensible or possible. The turbulence profiles were chosen to approximate the horizontally averaged measurements. They were considerably simplified and thus differ from the 'real' values at some stations within the canopy, but the LES results were not found to be very sensitive to these discrepancies.

The initial duration of the computations was over $100T$ ($T = h/u_*$), whereas the subsequent averaging duration for all the statistics was approximately 100T. Here $u_*$ is obtained from Xie and Castro (2008) for the inflow generation and can be considered as a mean friction velocity. As found by XC, the variations in statistical data throughout the roughness sub-layer (including the canopy region) were usually small once the averaging duration exceeded $20T$.

Since the data of temperature fluctuation statistics were not available, it is crucial to know whether the effect of the temperature fluctuations at the inlet on the velocity fluctuations and mean velocity is important. Subsequently a few numerical experiments were conducted and described as follows.

(I) The instantaneous temperature at the inlet was set as,

$$\theta(y,z,t) = \overline{\theta}(z), \tag{6}$$

where no temperature fluctuation was superimposed on the mean profile.

(II) Variance of the temperature fluctuations at the inlet was approximated by using the similarity relationship in surface layers under weakly stratified conditions (Stull, 1988, pp366), i.e. $\theta_{rms}/\theta_* \sim 2$, where $\theta_* = \overline{w'\theta'}/u_*$ is the surface layer temperature scaling parameter. Temperature fluctuations and heat fluxes measured at the BT Tower top and roof of the Westminster Council House on 03/06/2004 (Wood et al., 2009) were used as baseline for the approximation. It is to be noted that this is the data from case B ($\S4$). It was found that during 16:00-17:00 $\theta_{rms}/\theta_*$ was approximately 1.9 for the roof top data. A constant variance and the same mean temperature profile as in (I) were used to produce instantaneous temperature at the inlet,

$$\theta(y,z,t) = \overline{\theta}(z) + \theta'(y,z,t), \tag{7}$$

where the integral length scales of $\theta'$ was set equivalent to those of wall-normal velocity $w$.

(III) The instantaneous temperatures at the inlet were generated similarly as that in (II), except that the integral length scales of $\theta'$ were set equivalent to the averaged length scale of the velocities $u, v$ and $w$.

9

Fig. 3 (a,b) shows turbulence statistics profiles at station P1 behind row 7 (see Fig. 2) of the numerical experiments (I) and (II) at $R_b = -0.1$, and are compared with those in neutral conditions. The unstable thermal conditions enhance the velocity fluctuations evidently. Fig. 3 (a,b) also shows that the effect of the temperature fluctuations at the inlet on the velocity fluctuations, in particular the $w_{rms}$, is visible. However, the effects on the mean velocity profile seems very small (not shown). It was also noticed that the effect of the integral length scales of the temperature fluctuations at the inlet on the velocity fluctuations and mean velocity at station P1 behind row 7 is not significant, as long as reasonable length scales (e.g. in the order of the block size) were used. This is consistent with a conclusion for the length scales of turbulence in Xie and Castro (2008).

It is also of interest to check the effect on turbulence of the profile shape of the mean temperature at the inlet. Fig. 1(a) shows two different profiles of the dimensionless mean temperature specified at the inlet. Fig. 3(c,d) shows the stability effect of the shape of the mean temperature profile at the inlet on the velocity fluctuations at station *P*1 behind row 7. The effect on the velocity fluctuation *rms* is visible but is relatively small, whereas the effect on the mean velocity is hardly discerned (not shown).

Fig. 4 shows the stability effect of the approach flows on the mean velocity vectors $(U, W)$ on a vertical plane at P1 behind row 5. Fig. 4(a) (unstable) shows a larger circulation region in front of the cube than those in (b)(stable) and (c)(neutral). A 'calm' region with nearly zero velocity magnitude was found within a street-canyon under stable stratification condition with a Richardson number 0.79 based on the street canyon height and the mean velocity at the top of the street canyon (Uehara et al., 2000). Note in the present paper the bulk Richardson number $R_b$ was calculated based on the block height and the freestream velocity. A Richardson number based on the block height *h* and the mean velocity at the top of the canopy (which is similar as that for a street canyon in Uehara et al. (2000) ) would not be much different from 0.79 for the stable case in Fig. 4 (b). However, no such 'calm' region was found in flows over a group of staggered cubes under stable conditions with $R_b$ up to 0.2. This suggests that the effect of the stable thermal condition on the flows over staggered cubes are quite different from those for street canyons. These are probably due to the fact that for cube flows in weakly stable and neutral conditions, the flows are highly three dimensional and the scales of eddies within and immediately above the canopy are dominated by the cube size. In unstable condition (i.e. $R_b$ = -0.2), the velocity magnitude in the region immediately behind cube was slightly greater than those for and $R_b = 0$. On the contrary, the difference of the mean flow field between Fig. 4(b) and (c) is

10
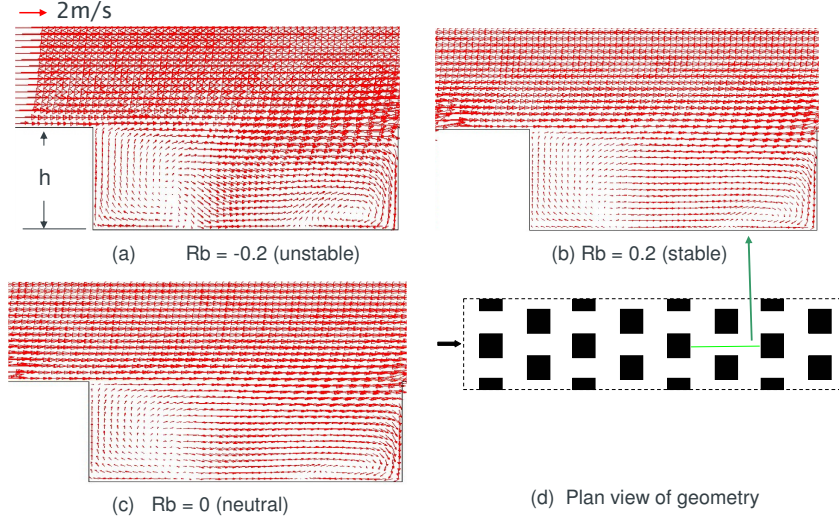
Figure 4: Mean velocity vectors (UW) on a vertical plane marked in (d) under various stratification conditions. (a) $R_b$ = -0.2; (b) $R_b = 0.2$ and (c) $R_b$=0.(d) plan view of the domain.

hard to discern.

We also found that the mean velocity vectors $(U,V)$ on a horizontal plane at half cube height show slightly stronger two counter circulations behind the cube under $R_b = -0.2$ than those under $R_b = 0.2$ and 0. This is consistent with Fig. 4 which shows that the unstable condition enhances the recirculation bubble in front of the cube. Fig. 5 shows velocity fluctuation *rms* and mean velocity at station $P1$ behind row 7, under various stratification conditions, i.e. $R_b$ = -0.2, -0.1, 0, 0.1 and 0.2. The turbulent fluctuation fields in the unstable conditions differ evidently from that in the neutral condition. However, the fluctuation fields in stable conditions show only a small difference compared with those in the neutral condition. Again, this is probably due to turbulent flows being block-size dominant during weakly stable and neutral conditions. And the buoyancy is less effective to suppress the turbulent motions than that in two-dimensional street canyon flows. The mean flow fields do not change evidently with the Richardson numbers.

The computational domain height in unstable conditions is more likely a concern than in neutral or stable conditions. A larger domain with a height $10h$ but other settings same as those in Fig. 2 was designed to test the effect of domain size. Fig. 5 shows that the velocity fluctuation *rms* and the mean velocity at $R_b = -0.2$ for the larger domain are slightly greater than those for the smaller domain.

11
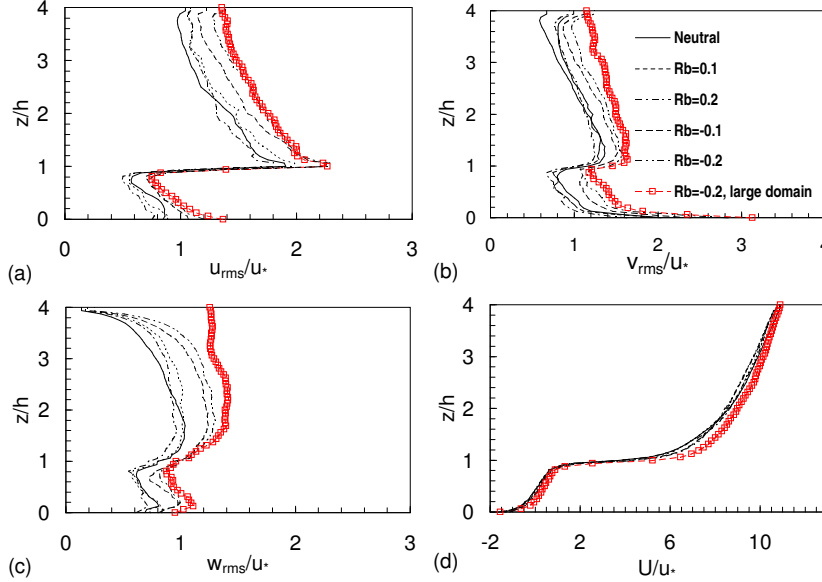
Figure 5: Velocity fluctuation *rms* and mean velocity at station $P1$ behind row 7, under stratification conditions $R_b$ = -0.2, -0.1, 0, 0.1 and 0.2. 'large domain', domain height $10h$.

Hanna et al. (2002) and Xie and Castro (2008) suggest that at stations behind row 7 (i.e. $x \sim 14h$), the flow field is fully converged. We noticed that at $x \sim 14h$ the temperature field seemed converged too. These results also suggests that the domain height $10h$ might produce a more accurate results than that $4h$, but at a cost of more grid points.

## 4. Flow and dispersion over DAPPLE site - Case B

Urban dispersion experiments in central London were carried out in the DAP-PLE project (Arnold et al., 2004; Wood et al., 2009). The DAPPLE project was focussed on the intersection between Marylebone Road and Gloucester Place (Dobre et al., 2005; Balogun et al., 2010) using full-scale dispersion experiments and micro-meteorological data. DAPPLE's methods are that an inert and passive tracer gas is released from a fixed point, and the gas is sampled at various stations in the near-field. In the present paper we use data from two field experiments. First, on 15th May 2003 at 17:00 local time (Martin et al., 2010a). Second on 3rd June 2004 at 16:30 local time (Martin et al., 2010b). The time-resolved experiments were such that the release was for 15 minutes, concurrent with sampling for 30

12

**Low resolution model (1:200)**
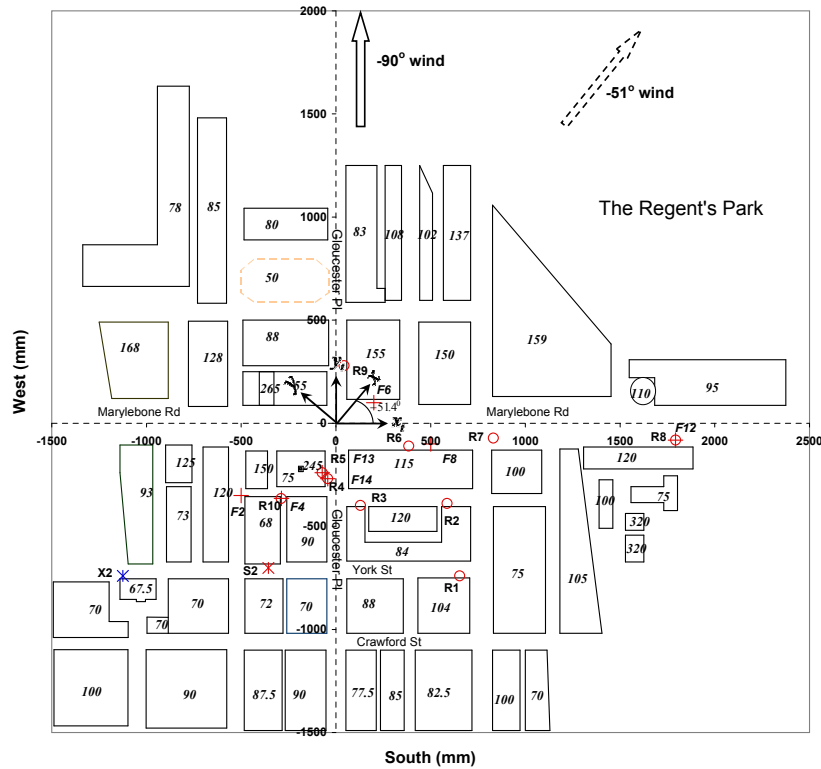


Figure 6: Plan view of the wind tunnel model. Numbers in italics on blocks indicate heights in mm. $S2$ and $X2$ are model and field sources respectively. $R1 - R10$ are sampling stations in a steady wind (§4.1). $F2$, $F4$, $F6$, $F8$, $F12$, $F13$ and $F14$ are sampling stations in a realistic wind (§4.2). The model coordinates are marked in mm, with $x_t$ from west to east, $y_t$ from south to north and $z$ from ground to top respectively. $x, y, z$ are the computational coordinates (Fig. 7).
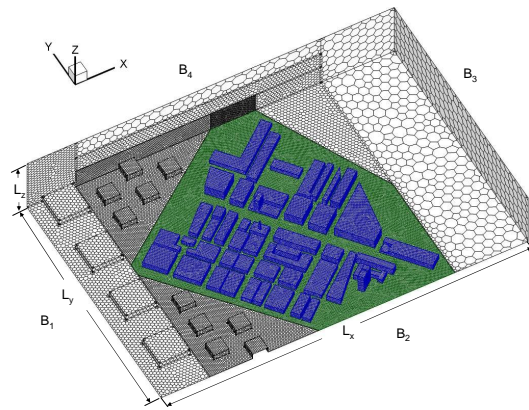


Figure 7: Computational domain with polyhedral mesh. The coordinate origin at the ground at the Marylebone Road - Gloucester Place intersection. $L_x$ =6000 mm, $L_y$ = 4000 mm, $L_z$ = 1000 mm in model scale.

13

minutes (i.e. continuing after release ends) of ten 3-minute samples.

For LES inlet flow conditions, we use data from atop BT Tower. Micrometeorological measurements have taken place almost continuously from 2004 to present (Wood et al., 2010). BT Tower is about 1.5 km east of the DAPPLE site. The measurements are mounted on a lattice tower on top of the main structure to give a measurement at 190.3 m above ground (Barlow et al., 2011); thus the measurement height is about 9 times higher than the mean building height in the DAPPLE area. A Gill R3-50 sonic anemometer gave 10 Hz values of 3D winds and ultrasonic temperature (similar to virtual temperature): and thus fluxes of sensible heat and momentum can also be estimated from these data (for atmospheric stability estimation). Data were quality-controlled using standard micrometeorological procedures (Wood et al., 2010). Means (at 30-sec and 60-sec average) of those raw data were made for use with LES.

We simulated flow and dispersion over a wind tunnel model - the 1:200 low resolution model. A detailed description of the numerical model can be found in Xie and Castro (2009) and Xie (2011). To ensure a self-contained study, a brief description of the numerical model is given here. The plan view of the model is shown in Fig. 6. The arrows with solid line and with dashed lines indicate the $-90°$ wind and $-51°$ wind respectively. The wind direction is defined as the angle bearing clockwise to the Marylebone-Rd direction, i.e. $x_t$ in Fig. 6.

The domain size is $L_x = 6000$ mm, $L_y = 4000$ mm, $L_z = 1000$ mm (see Fig. 7), and is 1.2 km, 0.8 km and 0.2 km respectively in full scale. The mean height of the building blocks is $h = 110$ mm, and the packing density is 0.5. Except for a few tall buildings, one small tower and one dome, most of the buildings are essentially of cuboid shape with low and different heights. The arrangement of the building blocks is mainly in staggered and aligned patterns with intersections and 'T' junctions. A street canyon pattern is also evident and seems more dominant for south-north streets than for east-west streets.

Boundaries B1, B2 and B4 (see Fig. 7) were set as inlets for the realistic winds. For the $-51°$ wind only the boundary B1 was set as an inlet, while B2 and B4 were set as symmetric walls. At the inflow boundaries an inflow approach (Xie and Castro, 2008) with the same turbulence quantities as in Xie and Castro (2009) and Xie (2011) was used to generate turbulence fluctuations correlated in space and in time. Boundary B3 was set as an outlet. The upper boundary of the domain was set as a stress-free wall and the other boundaries were set as solid walls. The wind conditions (i.e. direction and magnitude) on 03/06/2004 were used as in Xie (2011). At every time step, we scaled the Reynolds stresses accordingly, based on the mean velocity magnitude. More detailed descriptions can be found
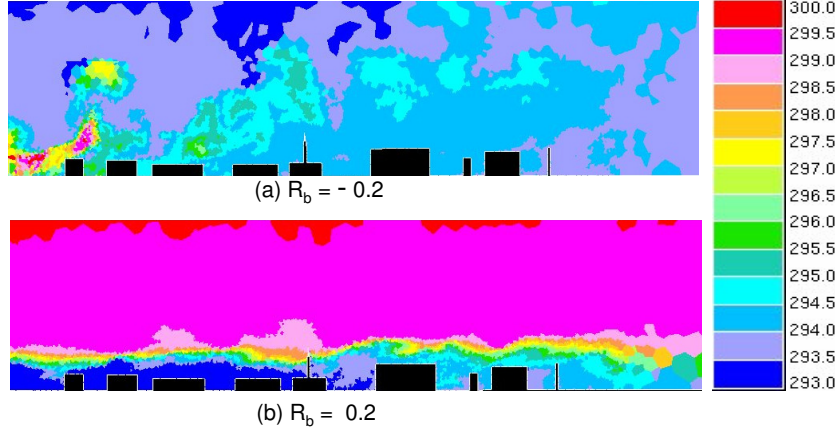
Figure 8: Instantaneous temperature contours (K) on a vertical ($x - z$ at $y = 0$) plane crossing the Marylebone Road and Gloucester Place intersection (defined as major intersection) in the $-51°$ wind. Wind direction is from left to right. (a)$R_b = -0.2$; (b)$R_b = 0.2$.

in Xie and Castro (2008, 2009). We generated the turbulence fluctuations at a plane normal to the wind direction in a local coordinate system based on the plane and then projected the velocities on the computational domain coordinate for inlet boundaries.

LES of dispersion in the $-51°$ and $-90°$ winds was validated and reported in Xie and Castro (2009) and Xie (2011) using wind tunnel data. In the present paper, dispersion in the $-51°$ and $-45°$ winds in various thermal stratification conditions was simulated and validated. Xie (2011) also reports LES of dispersion in realistic winds under neutral conditions. In order to investigate the effects of the thermal stratification in realistic winds, a few numerical experiments were conducted in the paper.

## 4.1. Flows and dispersion in steady winds

Large-eddy simulations and wind tunnel experiments were performed to investigate effects of thermal stratification on flows and dispersion in DAPPLE site in steady $-51°$ and $-45°$ winds. No temperature fluctuation was superimposed on the mean temperature at inlet in LES. Again since only weak stratification was considered, turbulence quantities at the inlet were set as those in a neutral condition (Xie and Castro, 2009).

Fig. 8 shows instantaneous temperature contours on a vertical ($x - z$, at $y = 0$)

15
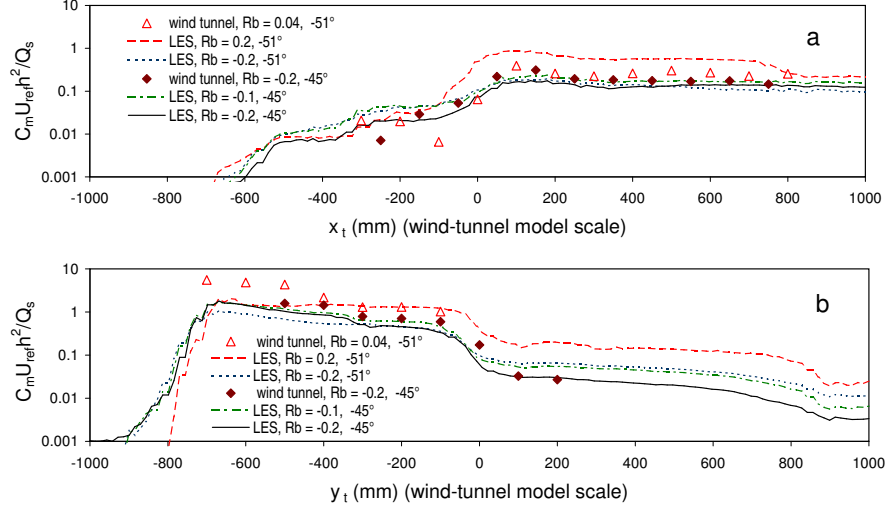
Figure 9: Non-dimensionalised mean concentration at height $z/h_m = 0.1$ along (a) Marylebone Road ($y_t = 0$) and (b) Gloucester Place ($x_t = 0$) in various thermal stabilities. $U_{ref}$ is the free-stream velocity. $Q_s$ is the concentration flux at the source. $h$ is the mean building height. Abscissa in wind tunnel model scale.

plane crossing the major intersection in unstable ($R_b = -0.2$) and stable ($R_b = 0.2$) conditions in the $-51°$ wind. It is to be noted that the distance from the inlet to the major intersection is $27h$. Such a distance is sufficient for flow and temperature fields to be fully developed within and immediately above the canopy, as discussed in §3. This is confirmed again in Fig. 8 (note the major intersection is immediately downwind of the council tower). It is also noted that the temperature field converges earlier in the stable condition (Fig. 8b) than in the unstable condition (Fig. 8a).

In the wind tunnel experiments and large-eddy simulations, a non-reactive tracer was released from a steady ground-level point source $S2$ (Fig. 6) in a few stratification conditions, whereas in the field experiments the release duration was 15 minutes in one stratification condition. Fig. 9 shows a comparison of dimensionless mean concentration along Marylebone Road and Gloucester Place under various thermal stratification conditions between the wind tunnel measurements and LES data. A test of sensitivity of dispersion to wind directions was performed. This shows that dispersion is not insensitive to wind directions under non-neutral conditions, which is consistent with that under a neutral condition Xie (2011).

16
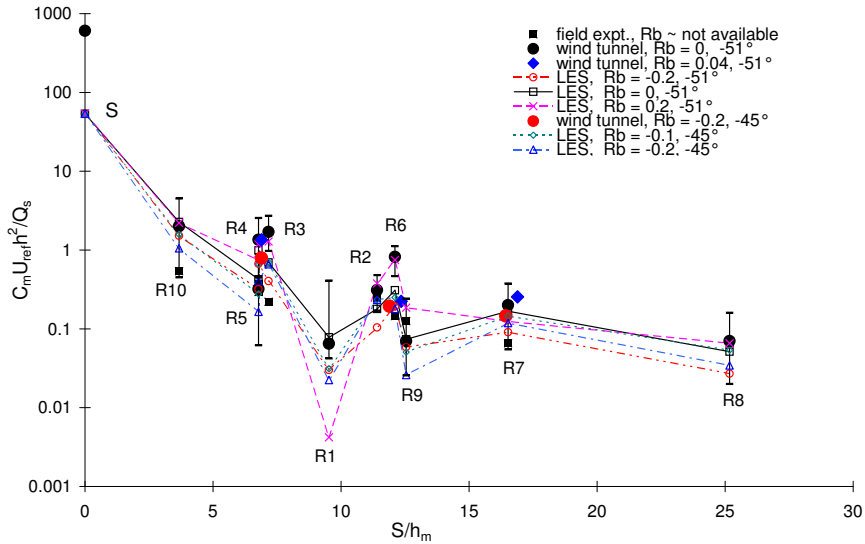
Figure 10: Non-dimensionalised mean concentration at stations $R1 - R10$ in various thermal stabilities. $U_{ref}$ is the free-stream velocity. $Q_s$ is the concentration flux at the source. $h$ is the mean building height. $S = |x_R - x_S| + |y_R - y_S|$ is the street distance to the source, where$(x_R, y_R)$ and $(x_S, y_S)$ are coordinates of the site and the source respectively.

Fig. 9 shows that case 'LES, $R_b$ = -0.2, -45°' is generally in better agreement with the measurements 'wind tunnel, $R_b$ = -0.2, -45°' than case 'LES, $R_b$ = -0.1, -45°'. This might suggest that the temperature inlet boundary conditions of LES is reasonable, even though the inlet temperature settings were not exactly identical as those in wind tunnel experiments. The mean concentration of case 'LES, $R_b$ = 0.2, -51°' is in large discrepancy with the measurements 'wind tunnel, $R_b$ = 0.04, -51°'. This is not surprising at all that the dispersion is sensitive to thermal stratification. Fig. 9 (a) shows almost constant mean concentration downstream of the major intersection ($x_t > 0$), which is due the channeling in Marylebone Road. A significant drop of concentration in Fig. 9 (b) and a significant increase in Fig. 9 (a) downstream of the major intersection ($x_t, y_t = 0$) under all of the stratification conditions suggest that the thermal buoyancy does not affect the major path (i.e. Gloucester Place - the major intersection - Marylebone Road) of scalar convection in these two winds.

Fig. 10 shows a comparison of dimensionless mean concentration at stations $R1$-$R10$. The field data were the maximum of 3-min bag concentration (Cheng and Robins, 2004). The concentration at site $R1$ varied dramatically at different

$R_b$ numbers, which was because $R1$ was located at the edge of the plume (see Fig. 6). The comparison between LES data and the corresponding wind tunnel measurements for a same $R_b$ in a same wind is promising. Recall that compared with the field measurements, LES using the realistic wind conditions in neutral conditions significantly improved the prediction at the near-field sites, but only marginally improved the prediction at the far field sites (Xie, 2011). Then it was suggested to include the thermal stratification in the LES. Due to lack of temperature measurements, a Richardson number for the 15/05/2003 field experiments is not presented in Fig. 10. Nevertheless, in general the wind tunnel and LES data under weakly unstable conditions are in better agreement with the field data than those under neutral or weakly stable conditions. This may suggest that the field experiments were conducted in a weakly unstable condition similar as that (e.g. $R_b \sim -0.1$) in §4.2.

### 4.2. Flows and dispersion in a realistic wind

Strictly speaking, the 'real' winds are never steady. However, we found so far that it was difficult to directly use weather data generated by operational numerical weather prediction models, e.g. the UK MetOffice's Unified Model, as boundary conditions to drive the street scale large-eddy simulations Xie (2011). Then we turned to using measured data with a high time resolution. Fig. 11 plots 30- sec averaged horizontal wind velocity from 16:00-17:00 on 03/06/2004, which was used to drive the LES. Fig. 6 also shows the source location $X2$ and the sampling stations $F2$, $F4$, $F6$, $F8$, $F12$, $F13$ and $F14$ of the DAPPLE field experiments on 03/06/2004. The LES was initialized at 16:00 with the source release switched on at 16:30 and off at 16:45, and with sampling and averaging started at 16:30 until 17:00.

Fig. 12 plots field measurements and six sets of LES results of 3-min averaged concentration at site $F14$ (the Westminster Council House doorway on west side of Gloucester Place by the major intersection) under four stratification conditions (i.e. $R_b = 0$, $-0.01$, $-0.03$, $-0.1$). In order to check the sensitivity of the initial conditions on the LES results, the two LES runs (i.e. run 1 & 2) under a neutral condition were initialised from different conditions. Fig. 12 shows that the effect of the initial conditions on the 3-min averaged concentration was not significant. Under the same stratification condition $R_b = -0.01$, the results with temperature fluctuations specified at the inlet were in good agreement with those with no temperature fluctuation at the inlet, which confirms that we observed in §3. For this reason, the inlet temperature in the other LES runs for the stratification conditions $R_b = -0.03$ and $-0.1$ were set with no fluctuations. Perhaps not
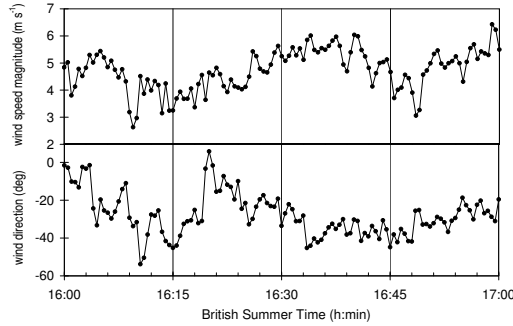
Figure 11: 30-sec averaged wind speed magnitude and direction (i.e. bearing clockwise to the Marylebone Road direction at BT Tower) on 03/06/2004. The source release was switched on at 16:30 and off at 16:45.

surprisingly, the 3-min averaged concentration decreases with the decrease of the Richardson number $R_b$. LES with $R_b = -0.1$ produced evidently less concentrations than the measurements, which suggests that specified $R_b = -0.1$ might be a bit less than the 'real' one in the field experiments, although we estimated that $R_b$ was approximately $-0.1$ at 16:00 on 03/06/2004.

Overall, the LES results for $R_b = -0.03$ and $-0.01$ are in marginally better agreement with the measurements than those for $R_b = 0$. The 'LES, $R_b = 0$, run1' and 'LES, $R_b = 0$, run2' data were fitted into a combined profile with two symmetric 'half Gaussian profiles' at the left and right end and a constant profile in the middle, where the constant is the maximum of the Gaussian profiles. The advection velocity of the plume was estimated using

$$U_{adv} = \frac{D}{T50}, \tag{8}$$

where $D$ is the distance from Site $F14$ to the source location $X2$, $T50$ is the elapsed time (since the release) when the ensemble-averaged concentration reaches 50% its local maximum at Site $F14$ (Cheng and Robins, 2004). Here $T50$ was estimated to be approximately 5 minutes and the advection velocity $U_{adv}$ is about $0.15U_{ref}$, which is close to the value $0.16U_{ref}$ suggested in Cheng and Robins (2004), who performed wind tunnel experiments in steady and neutral wind conditions. In Xie (2011) it is suggested that the advection velocity in varying wind is approximately the same as that in steady wind. Fig. 12 suggests that the $T50$ under weakly unstable conditions is approximately the same as that in neutral conditions.

Fig. 13 presents field measurements and LES results of 30-minute averaged

19
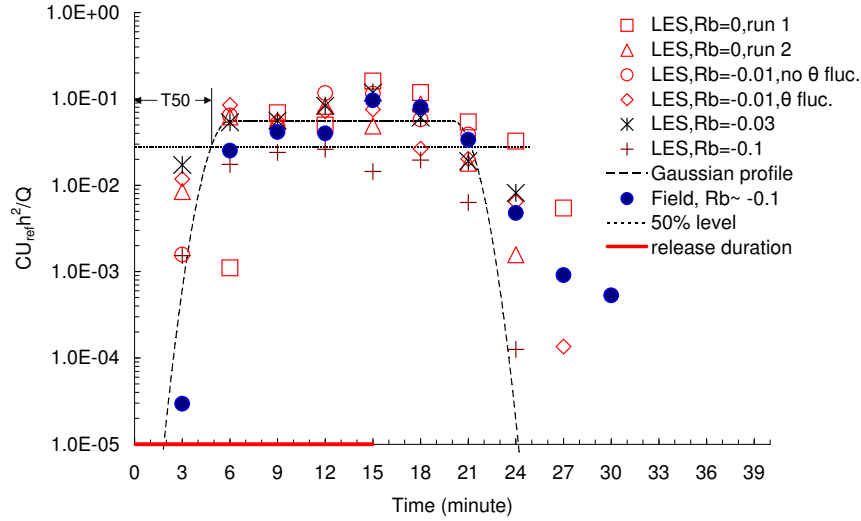
Figure 12: 3-min averaged concentration at field site $F14$ under various stratification conditions. $U_{ref}$ free-stream velocity; $Q$ concentration flux at source; $h$, mean building height; red solid line: 15 minutes release duration; dashed line: approximate location and width of a plume in combined Gaussian form; dot line: 50% level of maximum of the Gaussian profile; T50, approximate advection time.
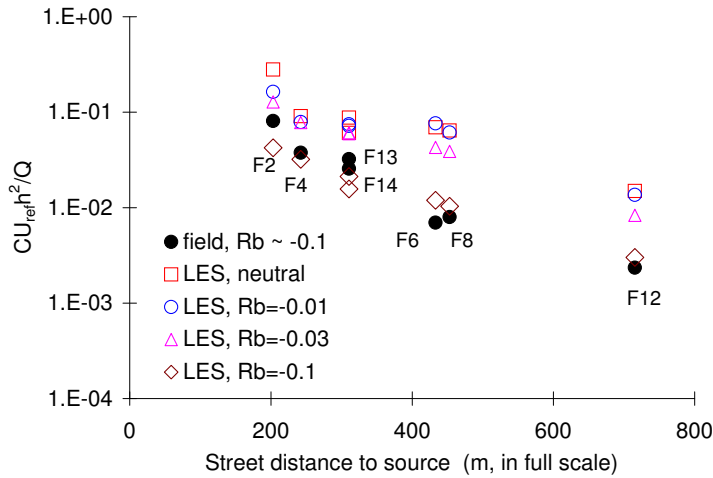


Figure 13: 30-min averaged concentration at the field sites $F2$, $F4$, $F6$, $F8$, $F12$, $F13$ and $F14$. $U_{ref}$ is the free-stream velocity; $Q$ is the concentration flux at source. $h$ is the mean building height. Street distance is defined as $S = |x_F - x_S| + |y_F - y_S|$, where $(x_F, y_F)$ and $(x_S, y_S)$ are coordinates of the site and the source respectively.

20

concentration at the 'F' sites. The averaging was started at 16:30 (when the release was switched on) until 17:00. LES data for the '$R_b$ = -0.03' are evidently less than those for the 'neutral', but still greater than the field measurements, in particular in the far field. LES data for the '$R_b = -0.1$' are significantly improved and are overall in the best agreement with the field measurements at the 7 sites. However, in the near field, i.e. $F2$, $F4$, $F13$ and $F14$, LES slightly under-predicted the 30-minute averaged concentration, which is consistent with Fig. 12 and again suggests that $R_b = -0.1$ might be a bit less than the 'real' one in the field experiments.

It was found that contours of 30-min averaged concentration at $z = 2$ m (in full scale) show a greater upwind and lateral spreading of the plume for the case '$R_b = -0.1$' than those for the neutral case, which is certainly due to stronger mixing within the canopy under unstable conditions. It was also noticed that the vertical spreading was much greater for the case '$R_b = -0.1$' than that for the neutral case. These confirm in Fig. 13 that the LES-predicted mean concentration for the '$R_b = -0.1$' is much lower than those for the neutral case at the 7 sites.

In summary, we should be cautious to interpret these LES results. First, a constant temperature within the canopy is not a small assumption, which might exaggerate the thermal effects or an effectively high $|R_b|$ number was used. Nevertheless, numerical experiments using various $R_b$ numbers have provided some more confidence for this assumption. In both LES calculations and wind tunnel experiments, the local thermal effects due to heat transfer through building and ground surfaces in the DAPPLE site were ignored. This produced an uncertainty for the comparison between the LES and the wind tunnel measurements and the field data.

## 5. CONCLUSIONS

In addition to considering the effects of inflow turbulence and weather-scale wind variation on dispersion in urban areas as in Xie and Castro (2009) and Xie (2011), effects of thermal stratification on dispersion were investigated using large-eddy simulations (LES). Firstly, flows over a group of staggered cubes under a few thermal stratifications, i.e. Richardson number $R_b = 0.2, 0.1, 0, -0.1$ and -0.2 were simulated. It was found that (1) the turbulent fluctuations and mean velocities were not affected substantially either by a change of the mean temperature profile below the canopy height or the temperature fluctuations at the inlet at the same $R_b$; (2) the effects on the flow field of the weakly unstable stratification conditions are greater than those of the weakly stable conditions at the same ab-

21

solute Richardson number $R_b$ for an array of staggered blocks. This was probably because under weakly stable conditions the flows were fully three-dimensional and the block-size scale was as dominant as that in the neutral conditions.

Secondly, the thermal stratification effects of the approach flows on turbulence and pollutant dispersion in DAPPLE site, central London was simulated. Based on an approximate estimation of the Richardson number $R_b \sim -0.1$ from the field data, a few Richardson numbers based on the average building height and freestream velocity, i.e. $-0.2 \le R_b \le 0.2$, of the approach flows were chosen for numerical experiments with adiabatic boundary conditions at the ground and building surfaces. We found that (1) under these weak stratification conditions, mean concentration at certain stations can be up to one order different from that in steady or varying winds in neutral conditions; (2) LES under unstable conditions significantly improve the numerical predictions of dispersion compared with that in neutral conditions. We conclude that stratification effects on dispersion even if under weakly unstable conditions in urban environments (e.g. in London) are not negligible. Further work, e.g. to consider the local heat transfer over solid walls, is being undertaken and will be reported in due course.

## References

Arnold S, ApSimon H, Barlow J, Belcher S, Bell M, Boddy D, Britter R, Cheng H, Clark R, Colvile R, Dimitroulopoulou S, Dobre A, Greally B, Kaur S, Knights A, Lawton T, Makepeace A, Martin D, Neophytou M, Neville S, Nieuwenhui-jsen M, Nickless G, Price C, Robins A, Shallcross D, Simmonds P, Smalley R, Tate J, Tomlin T, Wang H, Walsh P (2004) Introduction to the DAPPLE air pollution project. Sci Total Environ 332:139–153

Balogun A, Tomlin A, Wood C, Barlow J, Belcher S, Smalley R, Lingard J, Arnold S, Dobre A, Robins A, Martin D, Shallcross D (2010) In-street wind direction

variability in the vicinity of a busy intersection in central London. Bound-Layer Meteorol 136(3):489–513

Barlow J, Harrison J, Robins A, Wood C (2011) A wind-tunnel study of flow distortion at a meteorological sensor on top of the BT Tower, London, UK. Journal of Wind Engineering and Industrial Aerodynamics 99(9):899–907

Boppana VBL, Xie ZT, Castro IP (2010) Large-eddy simulation of dispersion from surface sources in arrays of obstacles. Bound-Layer Meteorol 135(3):433–454

Boppana VBL, Xie ZT, Castro IP (2012) Large-eddy simulation of heat transfer from a single cube mounted on a very rough wall. Bound-Layer Meteorol under review

Britter RE, Hanna SR (2003) Flow and dispersion in urban areas. Ann Rev Fluid Mech 35:469–496

Cheng H, Robins AG (2004) Wind tunnel simulation of field tracer release in London. In: Zhuang FG, Li JC (eds) Recent Advances in Fluid Mechanics, Tsinghua University Press & Springer-Verlag, pp 801–804

Dobre A, Arnold SJ, Smalley RJ, Boddy JWD, Barlow JF, Tomlin AS, Belcher SE (2005) Flow field measurements in the proximity of an urban intersection in London, UK. Atmos Environ, 39:4647–4657

Hanna SR, Tehranian S, Carissimo B, Macdonald RW, Lohner R (2002) Comparisons of model simulations with observations of mean flow and turbulence within simple obstacle arrays. Atmos Environ 36:5067–5079

Kanda M, Moriizumi T (2009) Momentum and heat transfer over urban-like surfaces. Boundary-Layer Meteorol 131::385–401

Liu HZ, Liang B, Zhu FR, Zhang BY, Sang JG (2003) A laboratory model for the flow in urban street canyons induced by bottom heating. Adv Atmos Sci 20:554–64

Louka P, Vachon G, Sini JF, Mestayer PG, Rosant JM (2002) Thermal effects on the airflow in a street canyon–Nantes'99 experimental results and model simulations. Water, Air, Soil Pollution: Focus 2:351–364

Martin D, Nickless G, Price C, Britter R, Neophytou M, Cheng H, Robins A, Dobre A, Belcher S, Tomlin JBA, Smalley R, Tate J, Colvile R, Arnold S, Shallcross D (2010a) Urban tracer dispersion experiments in London (DAPPLE) 2003: Field studies and comparisons with empirical prediction. Atmos Sci Lett 11:241–248

Martin D, Price C, White I, Nickless G, Petersson F, Britter R, Robins A, Belcher S, Barlow J, Neophytou M, Arnold S, Tomlin A, Smalley R, Shallcross D (2010b) Urban tracer dispersion experiments during the second DAPPLE field campaign in London 2004. Atmos Environ 44:3043–3052

Niceno B, Hanjalić K (2002) Turbulent heat transfer from a multi-layered wall-mounted cube matrix: A large eddy simulation. Int J Heat Fluid Flow 23:173–185

Pascheke F, Barlow JF, Robins A (2008) Wind-tunnel modelling of dispersion from a scalar area source in urban-like roughness. Boundary-Layer Meteorol 126:103–124

Richards K, Schatzmann M, Leitl B (2006) Wind tunnel experiments modelling the thermal effects within the vicinity of a single block building with leeward wall heating. J Wind Eng Ind Aerodyn 94:621–636

Stull RB (1988) An Introduction to Boundary Layer Meteorology. Kluwer Academic, the Netherlands

Tseng YH, Meneveau C, Parlange MB (2006) Modeling flow around bluff bodies and urban dispersion using large eddy simulation. Environ Sci Technol 40:2653–2662

Uehara K, Murakami S, Oikawa S, Wakamatsu S (2000) Wind tunnel experiments on how thermal stratifcation affects flow in and above urban street canyons. Atmos Environ 34:1553–1562

Wood CR, Barlow JF, Belcher SE, Dobre A, Arnold SJ, Balogun AA, Lingard JJN, Smalley RJ, Tate JE, Tomlin AS, Britter RE, Cheng H, Martin D, Petersson FK, Shallcross DE, White IR, Neophytou MK, Robins AG (2009) Dispersion experiments in central London: The 2007 DAPPLE project. Bull Amer Meteor Soc 90:955–969

Wood CR, Lacser A, Barlow JF, Padhra A, Belcher SE, Nemitz E, Helfter C, Famulari D, Grimmond CSB (2010) Turbulent flow at 190 metres above London during 2006-2008: a climatology and the applicability of similarity theory. Bound-Layer Meterol 137:77–96

Xie ZT (2011) Modelling of street-scale flows and dispersion in realistic winds - towards coupling with mesoscale meteorological models. Bound-Layer Meteorol 141(1):53–75

Xie ZT, Castro IP (2006) LES and RANS for turbulent flow over arrays of wall-mounted cubes. Flow,Turbulence and Combustion 76:291–312

Xie ZT, Castro IP (2008) Efficient generation of inflow conditions for large-eddy simulation of street-scale flows. Flow,Turbulence and Combustion 81:449–470

Xie ZT, Castro IP (2009) Large-eddy simulation for flow and dispersion in urban streets. Atmos Environ 43:2174–2185

Xie ZT, Hayden P, Voke P, Robins A (2004) Large-eddy simulation of dispersion: comparison between elevated source and ground level source. J Turbul 5(31):1–16

Yoshizawa A (1986) Statistical theory for compressible turbulent shear flows, with the application to subgrid scale modelling. Phys Fluids 29:2152–2164